FERMILAB-PUB-20-117-TD
ACCEPTED

Mechanical performance of the first two prototype 4.5 m long Nb_3Sn low-β quadrupole magnets for the Hi-Lumi LHC Upgrade

D.W. Cheng, G. Ambrosio, E.C. Anderssen, P. Ferracin, P. Grosclaude, M. Guinchard, J. Muratore, H. Pan, S.O. Prestemon, G. Vallone

***Abstract*—The U.S. High-Luminosity LHC Accelerator Upgrade Project (HL-LHC AUP) team is collaborating with CERN in the design and fabrication of the first 4.5 m long MQXFA magnets, a 150 mm aperture high-field Nb_3Sn quadrupole magnet that uses the aluminum shell-based bladder-and-key technology. The first two prototype magnets, MQXFAP1 and MQXFAP2, were assembled and tested while the first pre-series structure (MQXFA03) was in fabrication. This paper summarizes the mechanical performance of these prototype structures based on the comparison of measured strain gauge data with finite element model analyses from all load steps to powering. The MQXFAP1 magnet almost reached ultimate current before a short to ground was detected and the test was stopped. The MQXFAP2 magnet experienced a low training performance due to a fractured aluminum shell. MQXFAP1b was rebuilt with a new replacement coil, but an old coil limited the magnet from achieving the ultimate current. The mitigations and analyses of these prototype magnets are discussed in the context of the transition to pre-series production.**

***Index Terms*— Superconducting magnet, superconducting coils, High Luminosity LHC, MQXF, quadrupole, Nb_3Sn**

I. Introduction

THE development of high field Nb_3Sn magnets under the LHC Accelerator Research Program (LARP) [1] effort has resulted in the MQXF magnet [2], which is a Nb_3Sn quadrupole designed in partnership with CERN that will replace the present inner triplet quadrupoles of the LHC for the High Luminosity LHC project [3]. The MQXF design was scaled up from a series of technology development models [4]-[7] that used the bladder-and-key technology [8]. The short MQXF models (1.2 m long with a 150 mm aperture) are extensively reported on in [9]-[10], and its cross section is shown in Fig. 1. The MQXFA magnet is a 4.5 m (4.2 m magnetic length) length scale up of the same cross section that is being produced by the U.S. High-Luminosity LHC Accelerator Upgrade Project (HL-LHC AUP). These magnets also have the same cross-section as the 7.2 m long MQXFB [11] magnets being produced at CERN. Once MQXFA magnets are successfully tested, two of them will be installed together in a cold-mass, and subsequently inserted in a cryostat provided by-CERN.

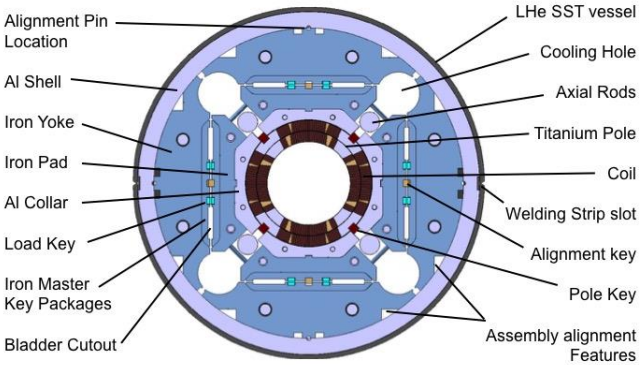

Fig. 1. MQXFA Cross section layout showing the main components. Note the LHe SST vessel is part of the cold mass.

To date, two MQXFA magnet prototypes have been assembled and tested in three iterations: MQXFAP1 (later referred to as MQXFAP1***a***) and MQXFAP1b, and MQXFAP2. The MQXFAP1a magnet reached nominal current in 9 quenches, but did not achieve the ultimate current level due to a short to ground that stopped the test campaign. Feedback from the test, however, along with data from the short models [10], helped to define the preload targets for MQXFAP2 magnet that was tested next. This second prototype exhibited low training performance that turned out to be caused by a fractured aluminum shell. A replacement coil was made for the first structure and

Manuscript submitted September xx, 2019. This work was supported in part by the U.S. Department of Energy, Office of Science, Office of High Energy Physics, through the U.S. LHC Accelerator Research Program (until 2018) and through the US HL-LHC Accelerator Upgrade Project (from 2018), and in part by the High Luminosity LHC project at CERN. The U.S. Government retains and the publisher, by accepting the article for publication, acknowledges that the U.S. Government retains a non-exclusive, paid-up, irrevocable, world-wide license to publish or reproduce the published form of this manuscript, or allow others to do so, for U.S. Government purposes. *(Corresponding author: Daniel W. Cheng.)*

D.W. Cheng (e-mail: dwcheng@lbl.gov), E.C. Anderssen, H. Pan, S.O. Prestemon, G. Vallone are with the Lawrence Berkeley National Laboratory, Berkeley, CA 94720 USA.

G. Ambrosio is with Fermi National Accelerator Laboratory, Batavia, IL 60510, USA.

J. Muratore is with Brookhaven National Laboratory, Upton, NY 11973, USA.

P. Ferracin, P. Grosclaude, M. Guinchard are with CERN, TE Dept. CH-1211 Geneva.

Color versions of one or more of the figures in this paper are available online at http://ieeexplore.ieee.org.

Digital Object Identifier will be inserted here upon acceptance.

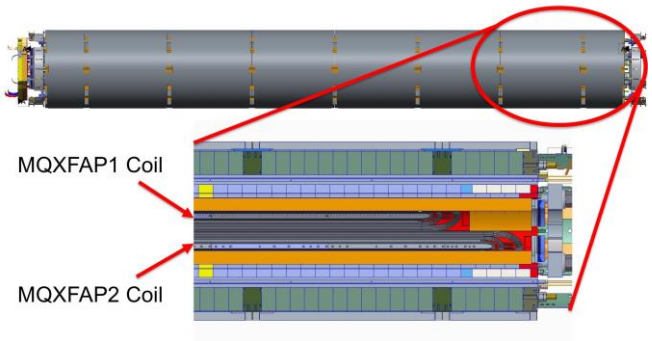

Fig. 2. Cross section detail of MQXFAP1 coil superimposed with a MQXFAP2 coil.

MQXFAP1b was assembled and tested. Although the new coil reached nominal current in 3 quenches, the magnet did not achieve the ultimate current because of a different limiting coil.

In this paper we report on the mechanical performance of these two prototype magnet structures with respect to the analytical models that predict their behavior. We also discuss the lessons learned from these assemblies, and finally present an outlook of the transition from assembling prototype magnets to pre-series magnets, which will be part of HL-LHC upgrade if they meet all requirements.

II. Prototype Magnets MQXFAP1 and MQXFAP2

A. Differences Between the Prototypes

MQXFAP1 is the first 4.5 m long prototype magnet, but incorporated 4.0 m magnetic length coils in the structure [12]. It has 1st generation coils, fabricated at FNAL and BNL with RRP 108/127 (1 coil), 132/169 (2 coils), and 144/169 (1 coil) conductor. MQXFAP2 shares the same cross section and structure length, but differs from the first prototype in that the coils have 4.2 m magnetic length, and the materials used in the structure are approved by CERN for use in the HL-LHC tunnel. See Fig. 2.

The yokes and shells of both structures had the same physical length, but the MQXFAP2 shells also incorporated a few changes based on feedback from the first magnet. First, the shells fabricator requested a 7075-T651 temper for the shell forging, which introduces a mechanical compressive stress-relief step between the quench and the aging steps. While this reportedly helps to maintain tight tolerances during machining, size constraints for this process limited this temper to only the shorter "end" shells; the longer "middle" shells remained 7075-T6 temper, according to the design, for this reason. Secondly, a small 3 mm radius was added to the cutouts of all the shells, which were sharp in the first prototype. These differences will be discussed later in this paper.

TABLE I
Comparisons of Azimuthal Preload Targets (MPa)

Cond.	Loc.	MQXFS1a	MQXFS1b	MQXFAP1	MQXFAP2	MQXFAP1b
R.T.	Coil	-61	-77	-75	-74	-69
	Shell	72	95	72	83	62
1.9 K	Coil	-81	-101	-88*	-91	-90
	Shell	140	173	140	153	130
Interference		460 µm	720 µm	640 µm	710 µm	510 µm
P.K. Gap**		0	0	50 µm	20 µm	70 µm

* Lost coil gauges during test; value is FEA result based on measured shell stress.
** Positive values indicate gap, negative values indicate interference.

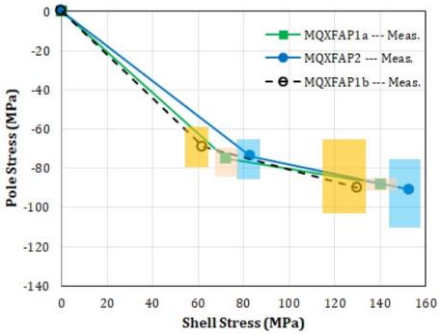

Fig. 3. Transfer function of the MQXFAP1 and MQXFAP2 magnets.

B. MQXFAP1 and MQXFAP2 Preload Targets

The assembly and preload targets of the MQXFAP1a were described in [12], based on experience at the time from the MQXFS1a/b models tested at FNAL[9], and the MQXFS3 model tested at CERN [10]. The magnet nominal operating current is 16.47 kA, and 17.89 kA is the maximum (ultimate) current that they will be qualified to. Table I shows the comparison of the azimuthal preload targets in several magnets. The azimuthal interference listed is determined by the fit of the magnet based on actual measurements, and it is the additional interference shim thickness added to achieve the target preload. The "pole key gap" is the per-side gap between the pole key and the collars (Fig. 1), and affects the shell stress for a given coil stress [12], because of the force intercepted by the key. See Fig. 3.

C. MQXFAP1a Strain Gauge Behavior During Testing

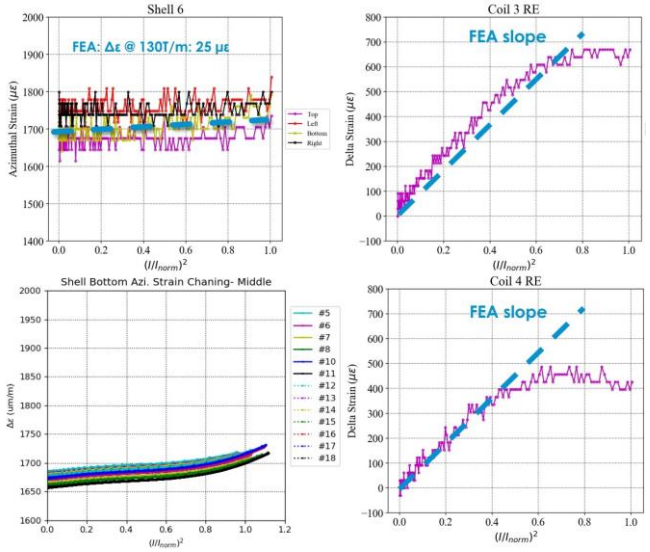

Fig. 4. Strain response (με) during Quench #10 (upper left) Shell 6, (upper right) Coil 03 azimuthal, (bottom right) Coil 04 azimuthal, and Shell 4 HBM (bottom left, multiple quenches).

MQXFAP1a was tested in the BNL vertical test facility and reported in [13] and [14]. The magnet experienced thermal cycles after the first and third quenches due to issues with the cryogenic system [13]. The magnet initially trained quickly—it had the highest first quench of the MQXF magnets to date, and took only 9 quenches to reach nominal current. Training behavior looked nominal compared with the MQXFS structures, showing some signs of plateauing. The magnet test was stopped due to a short to ground; a discussion of the findings and analyses can be found in [15].

Only a limited set of strain gauge data from the test was available due to the debonding of many gauges from the coils; only a few survived the thermal cycles. The limited coil data from Coils 03 and 04 showed slopes matching FEA models, however, there appeared to be an unloading of coil P04 at a relatively low current level at ~13 kA. See Fig. 4.

Rods strain gauges have historically been very reliable in the data they provided, even in the first long models using stainless steel rods [6]. However, the behavior of the

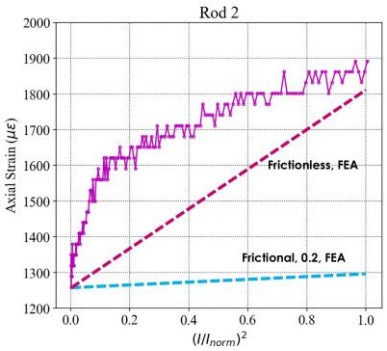

Fig. 5. Strain response (με) of axial Rod 2 during Quench #10 plotted against FEA scenarios.

MQXFAP1 rod gauges showed almost an order of magnitude higher strain that was not explainable at the time (and not physically possible, according to the FEA). See Fig. 5. The rod instrumentation was later changed for MQXFAP1b and will be further discussed in a later section.

D. MQXFAP2 Test Campaign

1) Low training performance

The second prototype, MQXFAP2, used 2nd generation coils with RRP 108/127 conductor that were fabricated at FNAL and BNL, 4.2 m long (magnetic length). The magnet had a first quench at 13.3 kA and reached 15 kA in 10 quenches, which were followed by detraining quenches. The training performance of the magnet is reported in [13] and [14]. All coils participated in the quenches, but the magnet was not able to reach the nominal current.

2) MQXFAP2 Mechanical Performance

Despite the poor training, however, the strain gauge data did not seem to indicate anything particularly wrong. Preload targets for the MQXFAP2 are also listed in Table I. One may notice that even though the preload of the coil was similar to that

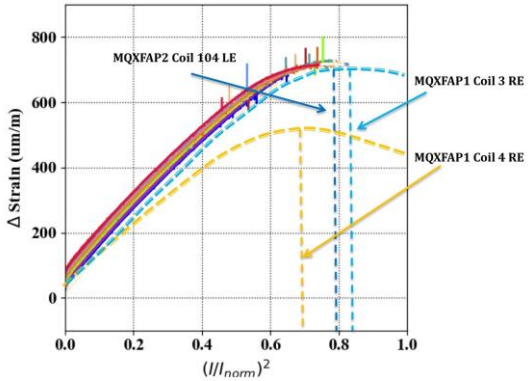

Fig. 6. Comparison of the coil azimuthal strain gauges; it appears that the preload of MQXFAP2 at least matches that of MQXFAP1.

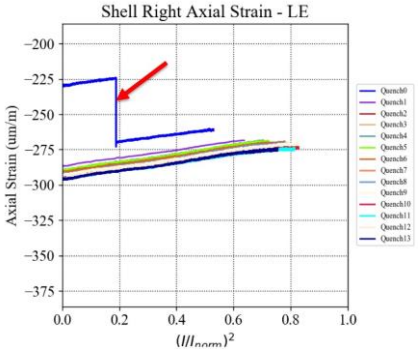

Fig. 7. Typical shell axial strain gauge response of the first 13 quenches including the first "0" current ramp, indicated by an arrow. The sudden drop of 50 με at about 7 kA was also visible in most strain gauges readings as well.

of MQXFAP1, a smaller pole key gap meant a higher shell stress was required to reach the target coil pole stress. Fig. 6 shows the comparison of the coil response with that of MQXFAP1, which appears to show that the coil azimuthal preload is at least as good as what had been achieved with the MQXFAP1 magnet.

Rod gauges also appeared to exhibit the same behavior as the MQXFAP1 magnet, roughly an order of magnitude higher response than the FEA models indicated.

3) A "Global" Event observed in the Strain Gauges

A study of the strain gauge data, however, indicated a "global" event that appeared in many strain gauge responses during an initial low current ramp prior to training. During this particular ramp, all the shell axial stations showed a sudden ~50 με drop at about 7 kA. See Fig. 7. This same event was also visible in the shell azimuthal gauges as well as many of the coil gauges too.

4) Shell Fracture

The test campaign was stopped after 26 quenches when it was clear the magnet performance would not improve. Upon removal from the cryostat the end shell on the non-lead-end was found to have split; see Fig. 8. A non-conformance had been reported and approved where sharp corners were machined on one end of this short "end" shell; such conditions had not detrimentally affected either the MQXFS or MQXFAP1 shells. At the time of fabrication, however, the Structural Design Criteria [16] had not yet been developed. These criteria, developed by AUP, are now requiring large radii (10 and 15 mm) at shell cut-outs, and require a detailed

Fig. 8. (L) Fractured shell on the non-lead-end of MQXFAP2. (R) Initiation of a crack from the sharp corner of a different quadrant of the shell.

analysis to verify safe operation [17] for non-conformities that may affect requirements.

Nonetheless, a crack likely initiated at the sharp corner as the shell stress increased during cooldown, and then it fractured upon the first current ramp. A more complete discussion of this can be found in [18] and [19]. The closest strain gauge stations to this shell were almost 1 m away, which would explain why the signals appeared to show no anomalies in the preload except for the "global event" that may have been the fracture, or a subsequent structure adjustment.

III. Rebuild of the MQXFAP1 Magnet

A. MQXFAP1b Preload Targets and Mitigations

After the low training performance of MQXFAP2 it was decided to fabricate a new (4.0 m magnetic length) coil to rebuild the MQXFAP1 magnet. This coil was fabricated conforming to the series coil production with the only difference being it was shorter in length.

Table I shows that a larger pole key gap (70 µm instead of 50 µm) was introduced in the assembly of this build to allow reduction of the shell stress by about 23 MPa at 1.9 K for the same target coil pole stress as before. Additional analyses on the shells were performed, studying in particular the ends of the magnet to ensure operation within safe margins. See Table II and Fig. 9. As a precaution, the five previously uninstrumented shell segments were also instrumented to serve as a shell fracture "indicator"—absolute strain values would not be obtainable from these, but they would respond definitively to a fractured shell.

<<Table. II here>>

<<Fig. 9 under Table II here at bottom of this column>>

All coil strain gauges were replaced, and two of the axial rods also had additional gauges installed on the non-lead-end, where the station would be less likely to see bending effects. As a control, the gauges on the lead-end also retained their gauges.

B. MQXFAP1b Structure performance

The magnet reached the nominal current of 16.49 kA in three quenches; all quenches were in Coil 06, the virgin coil, as expected. However, with the exception of one more quench in 06, all subsequent quenches were located in Coil 03, previously tested in MQXFAP1. The maximum current reached was 17.69 kA after 15 quenches and several fall backs [13]. Weak epoxy properties may have contributed to the limited coil performance, and an extensive campaign to study the properties of the impregnated epoxy have begun. A possible contributing factor may have been the pre-loading procedure, which was changed after this test, discussed in the next section.

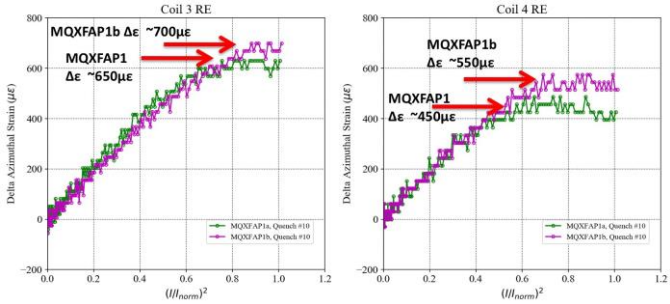

Fig. 10. Comparison of the MQXFAP1 and MQXFAP1b coil azimuthal strain for coils 03 (L) and 04 (R). Delta strain shown for comparison for quench #10.

Despite not reaching the ultimate current the data obtained from the strain gauges showed a good match to the FEA. Fig. 10 shows the coil azimuthal strain compared with the available data from MQXFAP1 magnet, which shows a higher delta strain before the turnaround occurred in MQXFAP1b, suggesting a higher preload.

Additionally, the data obtained from the re-positioned strain gauges for the axial rods showed a very good correlation to the FEA models, whereas the gauges on the opposite end continued to report an order of magnitude higher values. See Fig. 11.

Lastly, the shell gauges (both absolute and "indicator" gauges) also showed good correlation to the FEA models, and no indications of a broken shell.

<<Fig. 11 here at bottom of this column>>

IV. Lessons Learned

A. Implementation of Structural Design Criteria

It was fortunate that the MQXFAP2 shell fracture occurred while the shell forgings were in process for the MQXFA03 pre-series structure. The shells had not been machined at that time so the final machining was delayed in order to complete the analysis before proceeding. The development of the Structural Design Criteria for the MQXF shells and the graded approach to failure assessment [17] resulted in a few changes to the shells described in [18] that reduce stress concentrations to safe levels. These techniques can also be applied in the event any future shell non-conformities are reported.

A secondary method of reducing the shell stress is to also increase the poke key gap, which allows more force to be applied to the coils. For MQXFA03 a 100 µm gap was targeted, which will be adopted for the project if this magnet is accepted.

B. Magnet Preload Operations

Both MQXFAP1 and MQXFAP2 magnets were preloaded to the full azimuthal target before applying any axial preload. Some evidence from the short models and these two prototype magnets suggest that a path-dependent effect on the coil wedge-end spacer gap may be causing strand damage.

Starting with MQXFA03, the future magnets will have the axial plates in contact with the coil ends prior to applying any azimuthal preload. Then 50% of the azimuthal preload will be followed by 50% of the axial preload before applying the full azimuthal preload and finally finishing with the full axial preload.

V. Transitioning from Prototypes to Pre-Series

The first pre-series magnet, MQXFA03, was assembled by the time of submission, implementing the lessons learned from the prototypes. Testing will start in the Fall 2019.

Orders for the rest of the pre-series magnets parts (for structures 04-07) have already been placed, again with all the lessons learned applied, and the next magnet assembly will start also in the Fall 2019.

Additionally, a magnetic measurement system has been purpose-built for the MQXFA magnets, and magnetic and alignment measurements were performed on both prototypes. Results are reported in [20]-[21].

VI. Conclusion

In this paper we discussed the mechanical performance of the first two prototype MQXFA magnets for the HL-LHC AUP project, MQXFAP1 and MQXFAP2. The first magnet reached nominal current in 9 quenches, but did not achieve the ultimate current due to a short to ground. The second magnet did not reach nominal current due to a fractured shell. The rebuild of MQXFAP1b also did not reach ultimate current likely due to several factors possibly including weak epoxy in the limiting coil and the pre-loading procedure.

While the prototype magnets to date did not reach the maximum operating current, the lessons learned from these first two prototypes have been extremely useful and were applied to MQXFA03, the first of the pre-series magnets. They will be applied as well on the rest of the pre-series magnets, whose parts are presently being fabricated. MQXFA03 is slated for testing in Fall 2019.

Acknowledgment

The assemblies of the magnets would not be possible with the dedication and skill of Ahmet Pekedis, Joshua Herrera, Matt Reynolds, Tom Lipton, and Jordan Taylor. Additional support from the rest of our BCMT colleagues also cannot be overstated.

References

[1] S. A. Gourlay, *et al*., "Magnet R&D for the US LHC Accelerator Research Program (LARP)," *IEEE Transactions on Applied Superconductivity*, vol. 16, no. 2, pp. 324-327, June 2006.

[2] P. Ferracin, *et al.*, "Development of MQXF: The Nb_3Sn Low-ß Quadrupole for the HiLumi LHC," *IEEE Trans. Appl. Supercond.*, vol. 26, no. 4, June 2016.

[3] E. Todesco, *et al.*, "A First Baseline for the Magnets in the High Luminosity LHC Insertion Regions," *IEEE Trans. Appl. Supercond*. 24 (2014).

[4] H. Felice, *et al.*, "Test results of TQS03: a LARP shell-based Nb_3Sn quadrupole using 108/127 conductor," *Journal of Physics: Conference Series* 234 (2010) 032010.

[5] J. F. Muratore, *et al.*, "Test results of LARP 3.6 m Nb_3Sn racetrack coils supported by full-length and segmented shell structures," *IEEE Trans. Appl. Supercond.*, vol. 19, no. 3, pp. 1212–1216, Jun. 2009.

[6] G. Ambrosio, *et al.*, "Test Results and Analysis of LQS03 Third Long Nb_3Sn Quadrupole by LARP", *IEEE Trans. Appl. Supercond*., Vol. 23, No 3, June 2013.

[7] M J. DiMarco, *et al.*, "Test Results of the LARP Nb_3Sn Quadrupole HQ03a,", *IEEE Trans. Appl. Supercond*., Vol. 26, No 4, June 2016.

[8] S. Caspi, *et al.*, "The Use of Pressurized Bladders for Stress Control of Superconducting Magnets," *IEEE Trans. On Appl. Supercond.*, Vol. 11, No. 1 , March 2001.

[9] S. Stoynev *et al.*, "Summary of test results of MQXFS1—The first short model 150 mm aperture Nb_3Sn quadrupole for the high-luminosity LHC upgrade," *IEEE Trans. Appl. Supercond.*, vol. 28, no. 3, Apr. 2018, Art. no. 4001705.

[10] G. Vallone *et al.*, "Mechanical analysis of the short model magnets for the Nb_3Sn low-β quadrupole MQXF," *IEEE Trans. Appl. Supercond.*, vol. 28, no. 3, Apr. 2018, Art. no. 4003106.

[11] G. Vallone, *et al*., " Assembly of a mechanical model of MQXFB, the 7.2-m-long low-β quadrupole for the High-Luminosity LHC Upgrade," *IEEE Trans. Appl. Supercond.*, 29, 1-5, Aug. 2019.

[12] D. W. Cheng, *et al*., "Fabrication and Assembly Performance of the First 4.2 m MQXFA Magnet and Mechanical Model for the Hi-Lumi LHC Upgrade," *IEEE Transactions on Applied Superconductivity*, vol. 28, no. 3, pp. 1-7, April 2018, Art no. 4006207.

[13] J. Muratore, *et al*., "Test Results of the First Two Full-Length Prototype Quadrupole Magnets for the LHC Hi-Lumi Upgrade" *presented at this conference*.

[14] P. Ferracin, *et al*., " The HL-LHC Low-β quadrupole magnet MQXF: From short models to long prototypes," *IEEE Transactions on Applied Superconductivity*, vol. 29, no. 5, Aug. 2019.

[15] V. Marinozzi *et al.*, "Analysis of the heater-to-coil insulation in MQXF coils," *presented at this conference*.

[16] S. Prestemon, *et al*., "Structure Design Criteria", US-Hilumi DocDB #909.

[17] H. Pan, *et al*., "Failure Assessments for MQXF Magnet Support Structure With a Graded Approach," in *IEEE Transactions on Applied Superconductivity*, vol. 29, no. 5, pp. 1-7, Aug. 2019, Art no. 8401507.

[18] H. Pan, *et al*., "Fracture Failure Analysis for MQXF Magnet Aluminum Shells", *presented at this conference*.

[19] H. Felice, *et al*., "Report of the Review of the MQXFAP2 Al-Shell Issue and Lessons Learned", US-Hilumi DocDB #2192.

[20] H. Song, *et al*., "Vertical Magnetic Measurements of the First Full-Length Prototype MQXFAP2 Quadrupole for the LHC Hi-Lumi Accelerator Upgrade Project," in *IEEE Transactions on Applied Superconductivity*, vol. 29, no. 5, pp. 1-7, Aug. 2019, Art no. 4004707.

[21] H. Song, *et al*., " Vertical and High Current Magnetic Field Measurements of Full-Length MQXFAP Quadrupoles at Cryogenic Temperatures for Hi-Lumi LHC & PCB Rotating Coil Magnetic Field Measurement at BNL," *presented at this conference*.

TABLE II
STRESS (MPA) IN THE MQXFAP1B SHELLS UNDER DIFFERENT CONDITIONS

Location	1.9 K	16.47 kA	17.89 kA
Shell Avg. V.M. Stress at B	120	130	134
Shell Peak Stress at A	502	506	505

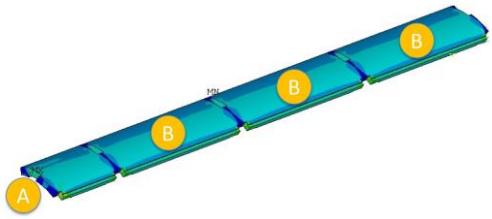

Fig. 9. (L) Octant model of the shells with areas of interest labeled. Circle A points to the end of the magnet, and Circle B is the middle of the shell. Refer to Table II.

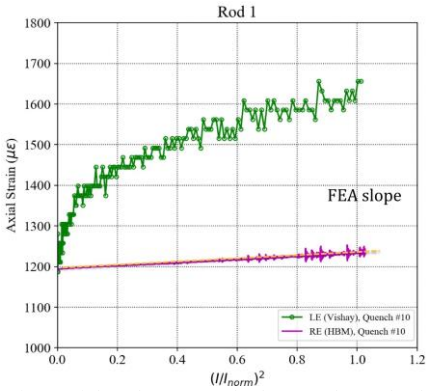

Fig. 11. Comparison axial Rod 1 gauges, both LE and Non-lead-end (spherical washer end). The non-lead-end matches the FEA result, whereas the Lead-end is an order of magnitude higher.